

Effect of annealing and B₄C diffusion barriers on the interfaces of Sc/Si periodic multilayers

Philippe Jonnard^{†,‡}, H el ene Maury^{†,‡}, Karine Le Guen^{†,‡}, Jean-Michel Andr e^{†,‡}, Nicola Mahne[§], Angelo Giglia[§], Stefano Nannarone^{§,¶}, Fran oise Bridou[§]*

([†]) Laboratoire de Chimie Physique - Mati ere et Rayonnement, UPMC Univ Paris 06, 11 rue Pierre et Marie Curie, F-75231 Paris cedex 05, France

([‡]) CNRS-UMR 7614, 11 rue Pierre et Marie Curie, F-75231 Paris cedex 05, France

([§]) Laboratorio Nazionale TASC, INFN-CNR, s.s.14, km 163.5 in Area Science Park, I-34012 Trieste, Italy

([¶]) Dipartimento di Ingegneria dei Materiali e dell'Ambiente, Universita di Modena e Reggio Emilia, Via Vignolese 905, I-41100 Modena, Italy

([§]) Laboratoire Charles Fabry de l'Institut d'Optique, CNRS, Univ Paris-Sud, Campus Polytechnique, RD128, F-91127 Palaiseau cedex, France

* philippe.jonnard@upmc.fr

Running title: X-ray reflectivity of Sc/Si annealed periodic multilayers

Corresponding author: Dr. P. Jonnard, Laboratoire de Chimie Physique - Matière et Rayonnement, 11 rue Pierre et Marie Curie, F-75231 Paris cedex 05, France ; tel : 33 1 44 27 63 03 ; fax : 33 1 44 27 62 26 ; e-mail : philippe.jonnard@upmc.fr

The optical properties of Sc/Si periodic multilayers are analyzed at three wavelengths in the x-ray range: 0.154, 0.712 and 12.7 nm. Fitting the reflectivity curves obtained at these three wavelengths enable us to constrain the parameters, thickness, density and roughness of the various layers, of the studied multilayers. Scattering curves were also measured at 12.7 nm on some samples to obtain an estimate of the correlation length of the roughness. Two sets of multilayers are used, with and without B₄C diffusion barrier at the interfaces. To see the efficiency of the B₄C layers the measures are performed after annealing up to 400°C. A dramatic change of the structure of the Sc/Si multilayer is observed between 100 and 200°C leading to a strong loss of reflectivity. For the Sc/B₄C/Si/B₄C multilayer the structure is stable up to 200°C after which a progressive evolution of the stack occurs.

KEYWORDS : multilayer, x-ray reflectivity, x-ray scattering, diffusion barrier, annealing, Sc, Si, B₄C

Introduction

In the 35-50 nm spectral range, the developments of new sources, such as discharge lasers¹ or harmonic generation sources², and the need for efficient mirrors for solar imagery³ have stimulated the interest in reflecting mirrors working at quasi-normal incidence at these wavelengths. In fact, single layer mirror whose best reflectivities are expected with Ir (20% at 50 nm and 5% at 35 nm) and Os (25% at 50 nm and 8% at 35 nm)⁴ are almost useless for long wavelength application. Thus, the use of periodic multilayers has been suggested and reflectivities ranging between 30-35% have been simulated for Os/Si, Ir/Si, Os/Al and Ir/Al systems,⁵ but the measured reflectivities did not exceed 20%. However, it has been shown that Sc/Si stacks have an important potential⁶ owing to the low absorption coefficient of Sc in the 35-50 nm spectral range. Later it was demonstrated experimentally^{7,8} that a reflectivity of the order of 50% can be obtained at 46 nm.

Despite its high measured reflectivity the Sc/Si system presents some problems. The Sc/Si interfaces are not stable and interlayers composed of silicide develop⁹⁻¹¹ during the deposition process, leading to an experimental reflectivity far below the predicted one. Upon annealing, the thickness and composition of the interlayers change and thus the reflectivity strongly decreases. To improve the thermal stability, thin films acting as diffusion barriers can be inserted between the Sc and Si layers. At first a layer of W, about 1 nm thick, was introduced as a diffusion barrier.¹²⁻¹⁴ The multilayer was observed to be stable up to a temperature of 200°C but the reflectivity was low due to the large absorption coefficient of tungsten. Cr has also been considered as a diffusion barrier¹⁵ but its stability is limited to 150°C. Then, boron carbide film, whose efficiency has been demonstrated for the Mo/Si system,¹⁶⁻¹⁹ was proposed as a diffusion barrier²⁰ and thermal stability demonstrated up to 300°C with 0,3 nm thick layers.⁸

In this paper, we characterize Sc/Si and Sc/B₄C/Si/B₄C systems by using x-ray reflectometry (XRR) in the hard (0.154 nm) and soft (0.712 nm) x-ray ranges. The properties of these multilayers are studied as a function of the annealing up to a temperature of 400°C. In the temperature range where large modifications of the samples occur, the results are completed by XRR measurements in the ultra-soft x-

ray range (12.7 nm) and x-ray scattering measurements.

Experimental methods

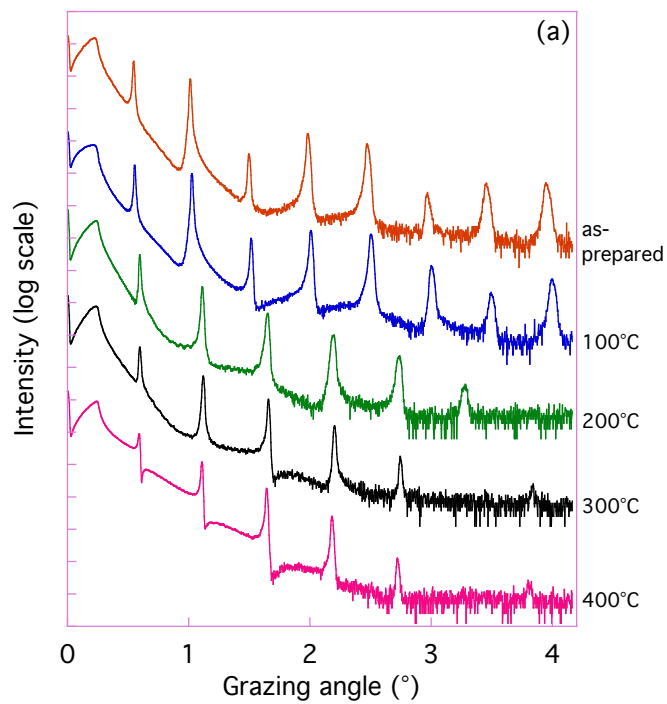
The Sc/Si multilayers are prepared by magnetron sputtering using argon as a sputtering gas in an apparatus described elsewhere.²¹ Samples are deposited on Si polished wafers. The thickness of the Si and Sc layers is 5 nm, leading to an aimed period of 10 nm. The number of periods is 40. The top layer is Si. Indeed, the use of Sc as final layer would result in a loss of reflectivity due to the oxidation of the metal layer.¹⁵ The Sc/B₄C/Si/B₄C samples are prepared in the same way, the thickness at the B₄C layer being 0.9 nm, leading to an aimed period of 11.8 nm. The samples are annealed during 1 h (this does not include the times for increasing and decreasing the temperature) under a residual argon atmosphere of 5 Pa. The annealing temperatures are 100, 200, 300 and 400°C. We call as-prepared samples, the samples that have not been annealed.

The samples are analyzed by specular optical reflectivity at three different wavelengths ranging from hard to ultra-soft x-rays: 0.154 nm (Cu K α emission at 8048 eV) performed with a grazing-incidence reflectometer,²² 0.712 nm (Si K α emission at 1740 eV) performed with a home-made spectrogoniometer²³ and close to the Si L edges at 12.7 nm (98 eV) with the reflectometer of the BEAR beamline²⁴ of the Elettra synchrotron facility. Indeed, for photon energies slightly lower than an absorption edge, relatively high reflectivities are expected. The diffuse scattering measurements are made with a radiation of 12.7 nm in the so-called transverse scan mode. The sample is rotated by $\pm 5^\circ$ with respect to the specular direction of the first Bragg peak, while the detector is kept at a fixed position. The goniometers used for the reflectivity measurements at 0.154, 0.712 and 12.7 nm have all about the same angular resolution of 0.001°.

Results

The reflectivity curves obtained at 0.154 nm are presented in Figure 1. In the studied angular range,

for the as-prepared samples, up to 8 diffraction orders are observed with the Sc/Si multilayer and 10 orders with Sc/B₄C/Si/B₄C one. Annealing at 200°C of the Sc/Si system suppresses the seventh and eighth Bragg peaks and shifts the peaks toward the large angles. For the Sc/B₄C/Si/B₄C system, these effects are less pronounced and noticeable at 400°C annealing temperature. Moreover in this case, the extinction of the third and sixth Bragg peaks is also observed, suggesting a variation of the division parameter of the multilayer (the ratio of the Sc thickness to the period).



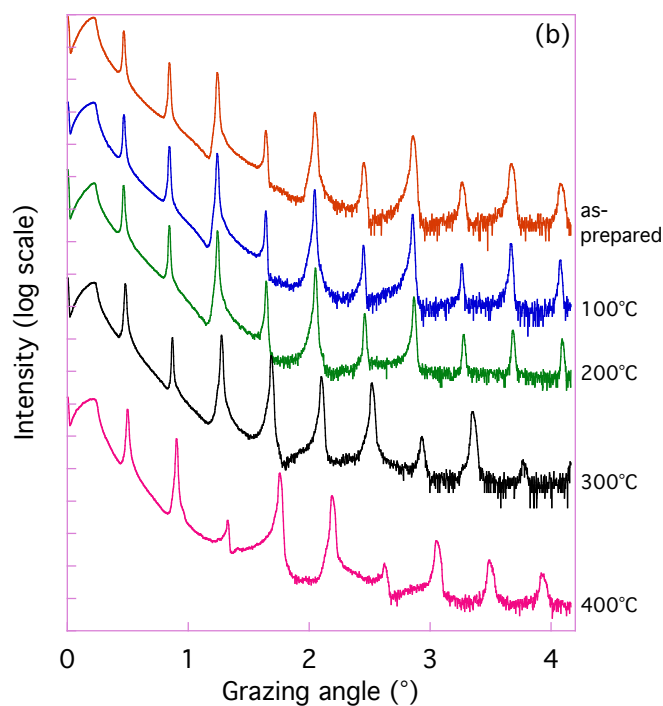


Figure 1. XRR curves measured at 0.154 nm for (a) the Sc/Si and (b) the Sc/B₄C/Si/B₄C multilayers, as-prepared and after annealing up to 400°C. The curves are shifted vertically for sake of clarity.

The shift of the Bragg peaks toward the high angles reflects a contraction of the period of the annealed multilayers. In order to show the different behavior of the Sc/Si and Sc/B₄C/Si/B₄C systems, we plot in the Figure 2 for each system the variation of the period with respect to the period of the non-annealed multilayer. This presentation is chosen because the two systems do not have the same original period. A sharp transition is observed between 100 and 200°C for Sc/Si, leading to a reflectivity decrease of about 10%. For Sc/B₄C/Si/B₄C, the decrease is only 3% at 300°C and 6.5% at 400°C.

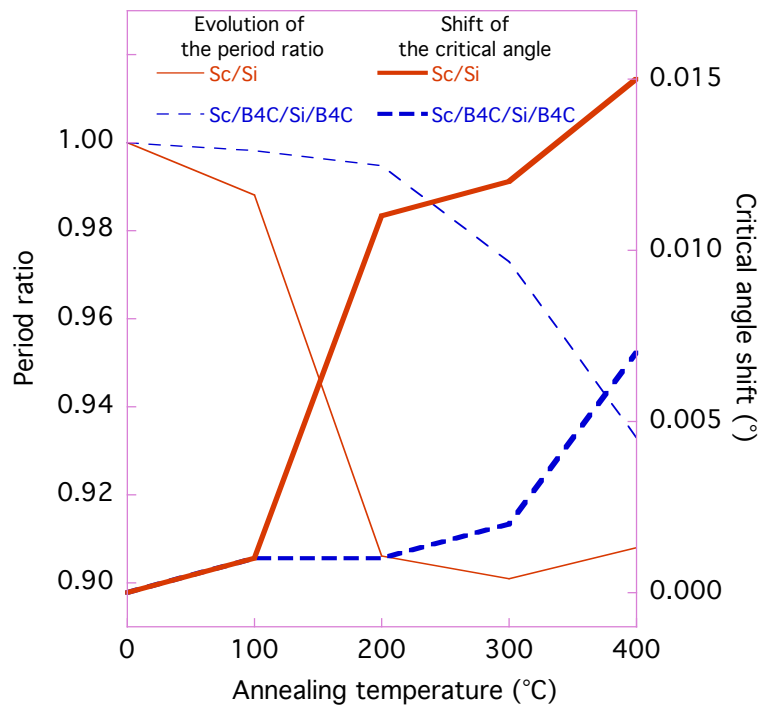


Figure 2. From the reflectivity curves measured at 0.154 nm and for the Sc/Si and the Sc/B₄C/Si/B₄C multilayers, evolution as a function of the annealing temperature of the ratio of the annealed multilayer period to the multilayer period of the as-prepared sample and shift of the critical angle for total reflection of the annealed multilayers with respect to the value corresponding to the as-prepared multilayer.

The variation of the period ratio is correlated to the variation of the critical angle for total reflection as shown in the Figure 2. Because the Sc/Si and Sc/B₄C/Si/B₄C as-prepared multilayers have different critical angles (0.251° and 0.245° respectively) we plot the shift of this angle for both systems as a function of the annealing temperature. For Sc/Si, a large shift is observed between 100 and 200°C; for Sc/B₄C/Si/B₄C the critical angle slightly increases up to 300°C, then a moderate shift is observed between 300 and 400°C. As the critical angle is sensitive to the overall composition of the samples, this means that there is much less chemical evolution in the Sc/B₄C/Si/B₄C multilayers than in the Sc/Si multilayers.

The contraction of the period is also observed in the reflectivity curves obtained at 0.712 nm. As an

example, Figure 3 presents the measurements obtained with the Sc/Si multilayer, as-prepared and annealed at 200°C, around the first Bragg peak. A high-angle energy shift of about 0.2° is observed accompanied by a reflectivity decrease by a factor greater than 5. The reflectivity variations also give information about the evolution of the multilayers. So we plot in the Figure 4 as a function of the annealing temperature the variation of the ratio of the reflectivity at a given temperature to the reflectivity of the non-annealed multilayers. The large decrease of the reflectivity of Sc/Si between 100 and 200°C is well correlated with the large period contraction observed in this temperature range (Figure 2). In contrast, the reflectivity of the Sc/B₄C/Si/B₄C system shows a small decrease (10%) despite the period contraction observed between 200 and 300°C.

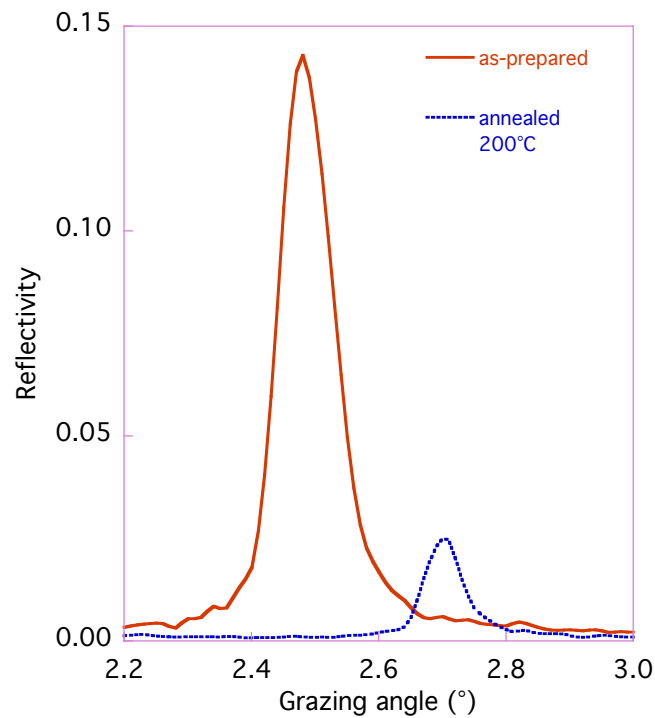


Figure 3. Reflectivity measured at 0.712 nm with the Sc/Si multilayer as-prepared and annealed at 200°C.

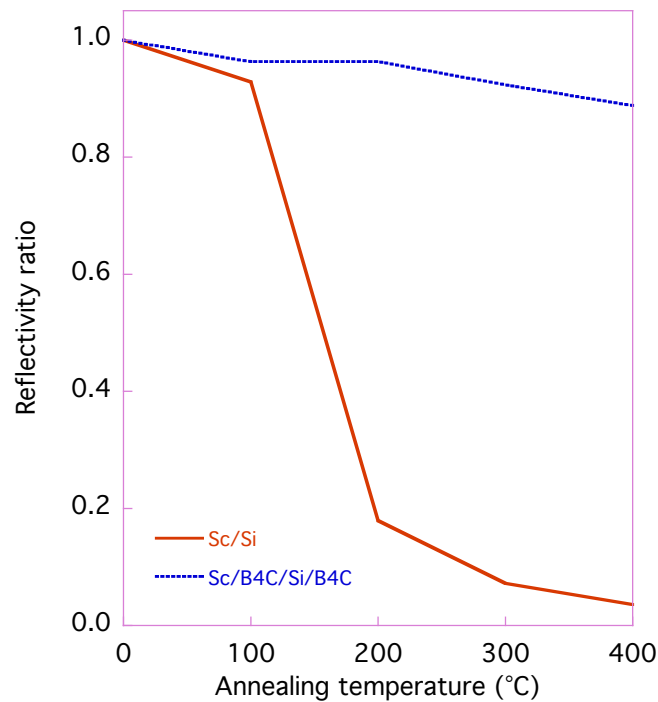


Figure 4. Evolution as a function of the annealing temperature of the ratio of reflectivity of the annealed multilayer to reflectivity of the as-prepared multilayer deduced from the reflectivity curves measured at 0.712 nm, for the Sc/Si and the Sc/B₄C/Si/B₄C multilayers.

We show in Figure 5 the reflectivity measurements obtained at 12.7 nm around the first Bragg peak for both systems as-prepared and annealed at 200°C. In agreement with the observation at the two other wavelengths, we observe a strong decrease of the reflectivity and large period contraction with the Sc/Si system, whereas a very small intensity decrease and almost no variation of the Bragg peak position is noted with the Sc/B₄C/Si/B₄C multilayer. The scattering intensity measurements around the first Bragg peak are presented on an absolute intensity scale in Figures 6a and 6b. It is observed that the scattered intensity decreased drastically outside the specular direction. In the case of Sc/Si, due to the period contraction and large variation of the reflectivity, it is not possible to directly compare the shape of the scattering curves as a function of the annealing temperature. Thus, for this system, we have normalized both scales as presented in Figure 6c: the angles are defined with respect to the specular direction

corresponding to the first Bragg peak and the intensities are normalized to unity. For the Sc/Si system, it is observed that the scattered intensity is more flat when the sample is annealed. The evolution of the shape of the scattering curve for the Sc/B₄C/Si/Si/B₄C system is more complex.

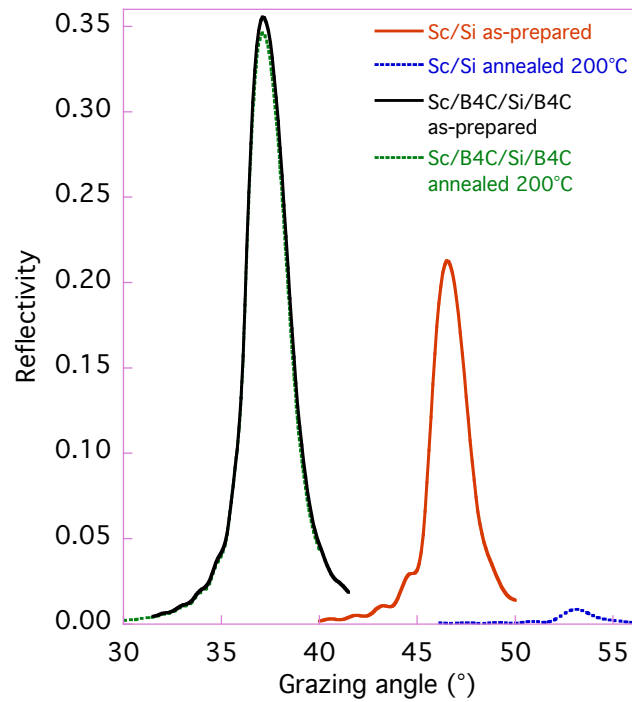


Figure 5. Reflectivity measured at 12.7 nm for the Sc/Si and Sc/B₄C/Si/B₄C multilayers, as-prepared and annealed at 200°C.

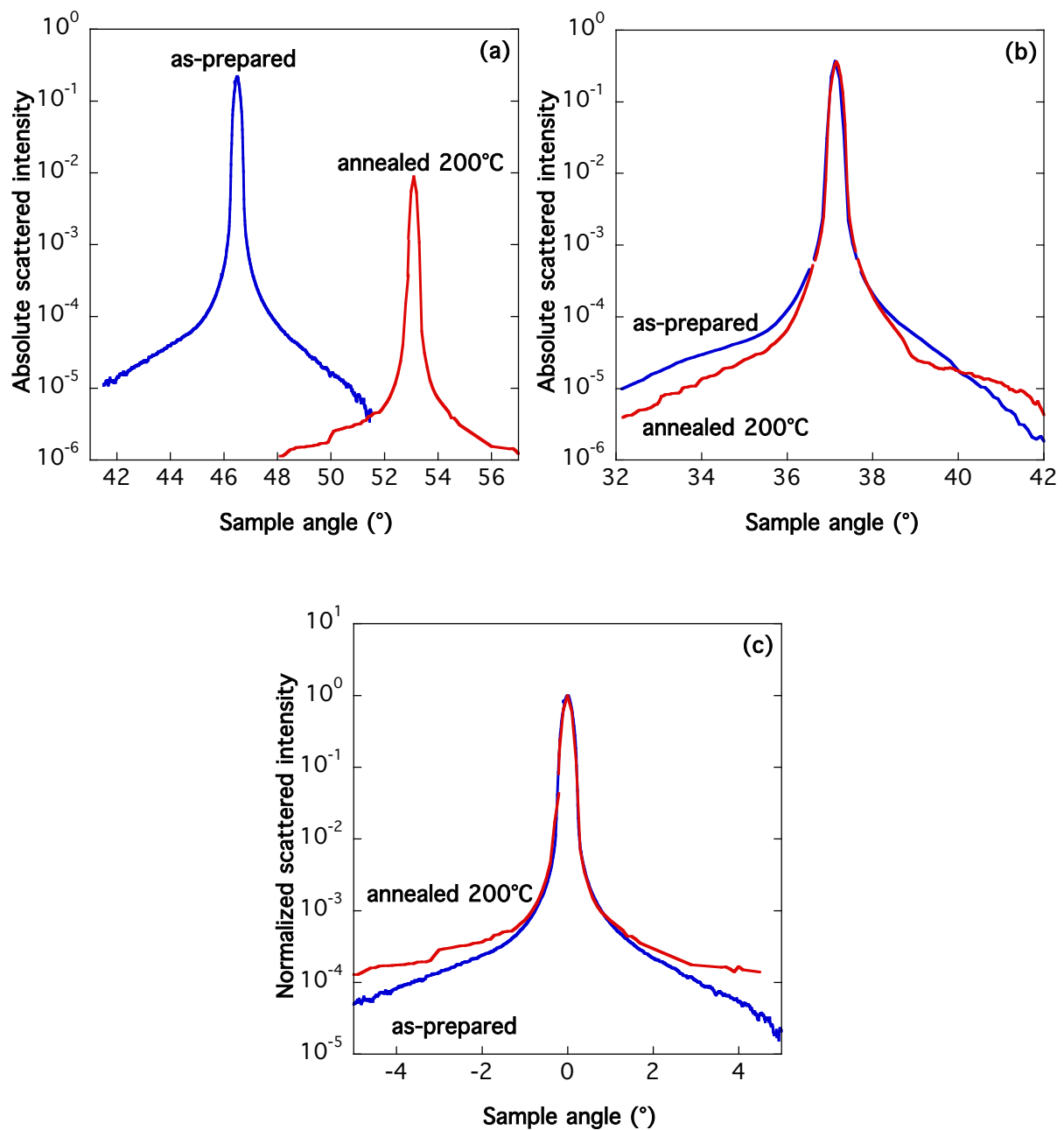


Figure 6. Scattering measurements obtained at 12.7 nm around the first Bragg peak of the (a) Sc/Si and (b) Sc/B₄C/Si/B₄C multilayers, as-prepared and annealed at 200°C. In (c) the same curves as in (a) are presented but on an angular scale relative to the position of the first Bragg peak and with normalized intensities.

Discussion

It is now well established that silicides develop at the interfaces of the Sc/Si multilayers.^{8,9,11,12,14,15,25}

The higher density of the silicide with respect to the densities of Sc and Si explains the period contraction of the multilayer. It has been determined by transmission electron microscopy, x-ray emission and absorption spectroscopies and XRR that the silicide is ScSi (whereas Sc₅Si₃ and Sc₃Si₅ can be also expected from the phase diagram²⁶⁻²⁹ as well as from thermodynamics considerations²⁸), that its thickness ranges from 1 to 3 nm depending on the preparation conditions and that the Sc-on-Si and Si-on-Sc interfaces can be asymmetrical. Thus in order to determine the parameters of the Sc/Si stacks, *i.e.* thickness, *rms* roughness height and refraction indices of the various layers, we have fitted the reflectivity curves by describing the sample with four layers within a period, *i.e.* Sc/ScSi/Si/ScSi. The fits are done with the constraint to obtain almost the same thickness of a given layer when fitting at the three different wavelengths. The maximum deviation between the three determinations is 0.1 nm and the presented value is their mean. This constraint is released for the roughness, because it is well known that different values of roughness are obtained at different wavelengths. However, only the mean roughness over the different wavelengths is presented.

As an example of fit we show in the Figure 7 the comparison of the XRR curves of the as-prepared Sc/Si sample obtained at 0.154, 0.712 and 12.7 nm and their fit. It is necessary to consider the last layer of the stack as SiO₂. At 0.154 nm, the overall experimental curve is well reproduced by the fit. It is not possible to reproduce accurately the intensity of the last Bragg peak, very probably due to a small irregularity of the period. This is confirmed by the broadening of the peaks toward the high angles. There is some discrepancy between the reflectivities measured and fitted at 0.712 nm. However, this difference is within the 5% of the estimated uncertainty on the experimental intensity measurements.²³ There is a very good agreement between the fit and the experimental results at 12.7 nm showing the consistency of the determined parameters of the stack.

The thickness and roughness determined for the Sc/Si samples are indicated in the Table I. The optical indices of the layers within the stacks have also been determined from the fits of the XRR curves. They show that the value of the index of the interlayers is close to what can be calculated from the Sc and Si

scattering factors for ScSi having the density of the bulk (3.3 g/cm^3). For the as-prepared and annealed at 100°C samples, the ScSi interphases are asymmetrical, the Sc-on-Si one being thinner than the Si-on-Sc one. There is no large difference between the samples as-prepared and annealed at 100°C . From the annealing temperature of 200°C , it is not necessary to consider the sample as a quadri-layer. Then, the reflectivity curve is fitted by a two-layer model of the multilayer: one Sc layer and one silicide (ScSi) layer in a period. The composition change is demonstrated by the large variation of the critical angle measured at 0.154 nm (Figure 2). It also leads to the period contraction (Figure 2) and to a strong loss of reflectivity (Figure 4) because the gap between the indices of the layers decreases. Between 200 and 300°C , the silicide content increases within the multilayer while the roughness stays in the same range. Due to the strong evolution of the sample, it is not possible to find a good fit of the 400°C curve. This results is in contrast with measurements by x-ray absorption and emission spectroscopies on the same samples¹¹ which indeed show that the formation of silicide is well underway at low annealing temperatures but detect the strong alteration of the sample only between 300 and 400°C . This discrepancy is not yet well understood but could be related to the fact that the spectroscopic methods are sensitive to the local order around the studied atoms whereas the reflectivity method relates to the long-range order.

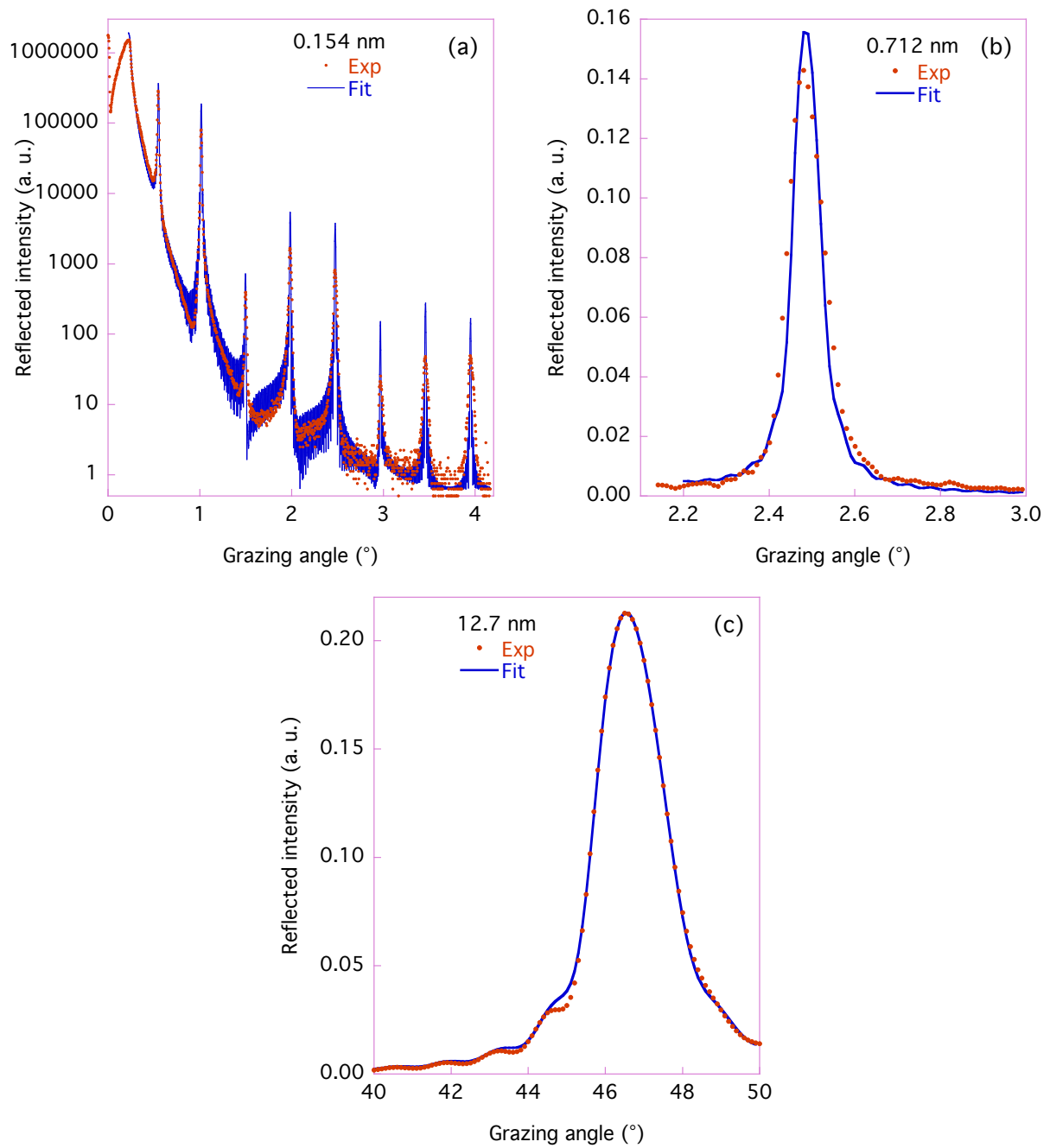


Figure 7. XRR curve measured at (a) 0.154, (b) 0.712 and (c) 12.7 nm of the as-prepared Sc/Si multilayer and fit by a stack having four layers in a period.

TABLE I. Parameters of the as-prepared and annealed Sc/Si multilayers deduced from the fit of the XRR curves obtained at 0.154, 0.712 and 12.7 nm using two or four layers in a period. For the samples as-prepared and annealed at 100°C, the fit is done by considering a multilayer with 4 layers in a period: Sc/ScSi/Si/ScSi. For the higher annealing temperatures, the fit is done by considering a multilayer with 2 layers in a period: Sc/ScSi.

Sc/Si Sample	Layer	Thickness (nm)	Roughness (nm)
As-prepared	Sc	3.00	0.30
	ScSi	2.00	0.34
	Si	2.84	0.39
	ScSi	1.13	0.36
Annealed 100°C	Sc	2.91	0.35
	ScSi	2.04	0.26
	Si	2.80	0.28
	ScSi	1.12	0.32
Annealed 200°C	Sc	2.00	0.52
	ScSi	6.15	0.53
Annealed 300°C	Sc	1.72	0.23
	ScSi	6.37	0.26

The thickness and roughness determined from the reflectivity curve of the as-prepared Sc/B₄C/Si/B₄C sample is indicated in the Table II. A thin SiO₂ layer at the surface is taken into account in all cases. It is not necessary to introduce some silicide at any interface. The thickness of the B₄C layers (0.8 nm) is slightly lower than the aimed one (0.9 nm). There is no significant difference neither between the curves nor between their fit, of the as-prepared and annealed at 100 and 200°C samples. This was not the case with the Sc/Si multilayer. In the case of the samples annealed at 300 and 400°C, there is a small but significant evolution of the reflectivity curves with respect to the ones obtained at lower temperatures. So one should consider Sc, Si, B₄C, silicide (reaction between the Sc and Si atoms), carbide (reaction between the Sc or Si atoms with the C atoms) or even boride (reaction between the Sc or Si atoms with

the B atoms) layers within a period. However from the x-ray emission and absorption spectroscopy measurements¹¹ performed at the Si L and Sc L edges, and giving informations about the chemical state of the Si and Sc atoms respectively from their valence states, the formation of silicide is excluded. In this study¹¹, it has been noted that a nitrogen contamination can take place in the Sc/B₄C/Si/B₄C samples. Thus the curves of the samples annealed at 300 and 400°C are not fitted because of the not precisely known structure of the stack.

TABLE II. Parameters of the as-prepared Sc/B₄C/Si/B₄C multilayers deduced from the fit of the XRR curves obtained at 0.154, 0.712 and 12.7 nm.

Layer	Thickness (nm)	Roughness (nm)
Sc	5.40	0.27
B ₄ C	0.80	0.29
Si	3.93	0.24
B ₄ C	0.81	0.34

To determine the effect of the annealing temperature on the correlation lengths of the roughness, the shape of the scattering curves has been fitted³⁰ using the IMD code. For these fits, the lateral correlation length, L , and the Hurst parameter or jaggedness factor, H , are set equal for all the layers. These parameters are introduced in the functional form of the correlation function of the roughness profile.³¹ The as-prepared Sc/Si sample can be fitted with a lateral correlation length of 22-24 nm, a perpendicular correlation length, Λ , of 5 nm (*i.e.* approximately the thickness of one layer) or 10 nm (*i.e.* approximately the thickness of one Sc/Si bi-layer) and a Hurst parameter of 0.1. As an example, the fit with $\Lambda = 5$ nm, $L = 23$ nm and $H = 0.1$ is shown in the Figure 8. Considering the Sc/Si multilayer annealed at 200°C, its fit leads to the same values of Λ and H but, as expected from the flatness of the curve, to a smaller value of L between 12 and 16 nm with respect to values deduced from the fit of the as-prepared sample.

It is much more difficult to find a fit for the Sc/B₄C/Si/B₄C multilayers. Indeed, their scattering curve is very asymmetrical, the high diffusion angle side being much steeper than its low side for the as-prepared sample and the reverse for the sample annealed at 200°C. Thus, it is not possible to find a fit for both sides of these scattering curves. If we consider only the low diffusion angle side, this leads to a large range of possible parameters that statistically describe the roughness: $\Lambda = 5-15$ nm, $L = 20-30$ nm and $H = 1.5-2.5$ for the as-prepared sample and $\Lambda = 5-15$ nm, $L = 25-35$ nm and $H = 0.15-0.25$ for the sample annealed at 200°C.

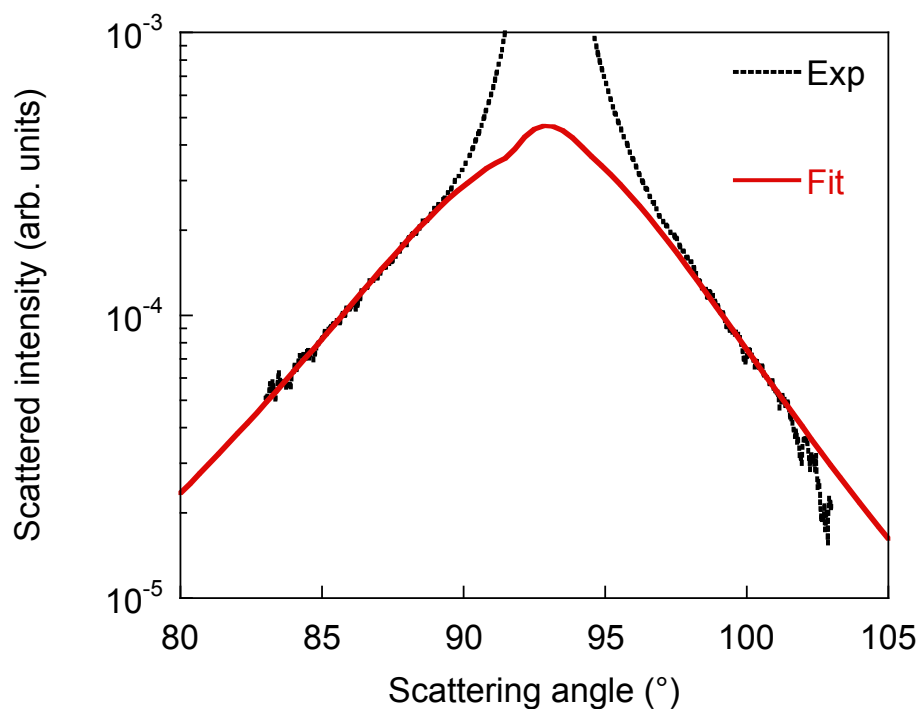


Figure 8. Diffuse scattering curve obtained at 12.7 nm around the first Bragg peak of the as-prepared Sc/Si multilayer and fit with a model taking into account a perpendicular correlation length of the roughness of 5 nm, a lateral correlation length of 23 nm and a Hurst parameter of 0.1.

Conclusions

It is shown for sample without annealing that the introduction of the barrier layers reduces the presence of the silicides at the interfaces and improves the optical performances at 0.712 nm. Upon annealing, the Sc/Si multilayer is stable only up to 100°C, after which a large decrease of the reflectivity

is observed together with an increase of interfacial silicides. For the Sc/B₄C/Si/B₄C multilayer, the optical reflectivity slightly decreases by 10% up to 400°C even if a 7% contraction of the period is determined and an evolution of the chemical state of the Si atoms between 300 and 400°C is detected. Diffuse scattering measurements measured on as-prepared and annealed at 200°C samples do not show a great influence of the annealing temperature on the correlation lengths of the roughness. Thus, the evolution of the optical performances of the studied stacks is mainly due to the development of the interfacial roughness and compounds.

Acknowledgments: Part of this work was supported by the European Community - Research Infrastructure Action under the FP6 "Structuring the European Research Area" Programme (through the Integrated Infrastructure Initiative "Integrating Activity on Synchrotron and Free Electron Laser Science") under contract RII3-CT-2004-506008 (IA-SFS). All multilayer depositions have been carried out on the deposition machine of CEMOX (Centrale d'élaboration et de métrologie des optiques X) implemented at the Institut d'Optique by PRaXO (Pôle d'optique des Rayons X d'Orsay).

- (1) Macchietto, C. D.; Benware, B. R.; Rocca, J. J. *Optics Letters* **1999**, *24*, 1115.
- (2) Constant, E.; Garzella, D.; Breger, P.; Mevel, E.; Dorrer, C.; Le Blanc, C.; Salin, F.; Agostini, P. *Physical Review Letters* **1999**, *82*, 1668.
- (3) Windt, D. L.; Donguy, S.; Seely, J.; Kjornrattanawanich, B.; Gullikson, E. M.; Walton, C. C.; Golub, L.; DeLuca, E. *Optics for EUV, X-Ray and Gamma-Ray Astronomy* **2004**, *5168*, 1.
- (4) Berreman, D. W.; Bjorkholm, J. E.; Becker, M.; Eichner, L.; Freeman, R. R.; Jewell, T. E.; Mansfield, W. M.; Macdowell, A. A.; Omalley, M. L.; Raab, E. L.; Silfvas, W. T.; Szeto, L. H.; Tennant, D. M.; Waskiewicz, W. K.; White, D. L.; Windt, D. L.; Wood, O. R. *Applied Physics Letters* **1990**, *56*, 2180.
- (5) Kozhevnikov, I. V.; Balakireva, L. L.; Fedorenko, A. I.; Kopealets, I. A.; Levashov, V. E.; Stetsenko, A. N.; Struk, II; Vinogradov, A. V. *Optics Communications* **1996**, *125*, 13.
- (6) Uspenskii, Y. A.; Levashov, V. E.; Vinogradov, A. V.; Fedorenko, A. I.; Kondratenko, V. V.; Pershin, Y. P.; Zubarev, E. N.; Mrowka, S.; Schafers, F. *Nuclear Instruments & Methods in Physics Research Section a-Accelerators Spectrometers Detectors and Associated Equipment* **2000**, *448*, 147.
- (7) Kaiser, N.; Yulin, S.; Feigl, T.; Bernitzki, H.; Lauth, H. *Proceedings of the SPIE - The International Society for Optical Engineering* **2004**, *5250*, 109.
- (8) Gautier, J.; Delmotte, F.; Bridou, F.; Ravet, M. F.; Varniere, F.; Roulliay, M.; Jerome, A.; Vickridge, I. *Applied Physics a-Materials Science & Processing* **2007**, *88*, 719.
- (9) Fedorenko, A. I.; Pershin, Y. P.; Poltseva, O. V.; Ponomarenko, A. G.; Sevryukova, V. S.; Voronov, D. L.; Zubarev, E. N. *Journal of X-Ray Science and Technology/Journal of X-Ray Science and Technology* **2001**, *9*, 35.
- (10) Voronov, D. L.; Zubarev, E. N.; Kondratenko, V. V.; Penkov, A. V.; Pershin, Y. P. *Funct. Mat.*

2002, 9, 534-539.

(11) Shendruk, T. N.; Moeves, A.; Kurmaev, E. Z.; Ochin, P.; Maury, H.; André, J.-M.; Le Guen, K.; Jonnard, P. *Thin Solid Films* in press. <http://dx.doi.org/10.1016/j.tsf.2010.01.036>

(12) Voronov, D. L.; Zubarev, E. N.; Kondratenko, V. V.; Penkov, A. V.; Pershin, Y. P.; Fedorenko, A. I. *Funct. Mat.* **1999**, 6, 856-859.

(13) Vinogradov, A. V.; Pershin, Y. P.; Zubarev, E. N.; Voronov, D. L.; Pen'kov, A. V.; Kondratenko, V. V.; Uspenskii, Y. A.; Artioukov, I. A.; Seely, J. F. *Proc. SPIE* **2001**, 4505, 230.

(14) Voronov, D. L.; Zubarev, E. N.; Kondratenko, V. V.; Pershin, Y. P.; Sevryukova, V. A.; Bugayev, Y. A. *Thin Solid Films* **2006**, 513, 152.

(15) Yulin, S. A.; Schaefer, F.; Feigl, T.; Kaiser, N. *Proceedings of the SPIE - The International Society for Optical Engineering* **2004**, 5193, 155.

(16) Bottger, T.; Meyer, D. C.; Paufler, P.; Braun, S.; Moss, M.; Mai, H.; Beyer, E. *Thin Solid Films* **2003**, 444, 165.

(17) Patelli, A.; Ravagnan, J.; Rigato, V.; Salmaso, G.; Silvestrini, D.; Bontempi, E.; Depero, L. E. *Applied Surface Science* **2004**, 238, 262.

(18) Maury, H.; Jonnard, P.; André, J. M.; Gautier, J.; Roulliay, M.; Bridou, F.; Delmotte, F.; Ravet, M. F.; Jérôme, A.; Holliger, P. *Thin Solid Films* **2006**, 514, 278.

(19) Maury, H.; Jonnard, P.; André, J. M.; Gautier, J.; Bridou, F.; Delmotte, F.; Ravet, M. F. *Surface Science* **2007**, 601, 2315.

(20) Jankowski, A. F.; Saw, C. K.; Walton, C. C.; Hayes, J. P.; Nilsen, J. *Thin Solid Films* **2004**, 469, 372.

(21) Yulin, S. A.; Kuhlmann, T.; Feigl, T.; Kaiser, N. *Proceedings of the SPIE - The International Society for Optical Engineering* **2002**, 4782, 285.

(22) Nevot, L.; Pardo, B.; Corno, J. *Revue De Physique Appliquee* **1988**, 23, 1675.

(23) André, J. M.; Avila, A.; Barchewitz, R.; Benbalagh, R.; Delaunay, R.; Druart, D.; Jonnard, P.; Ringuenet, H. *European Physical Journal, Applied Physics* **2005**, 31, 147.

(24) Nannarone, S.; Borgatti, F.; DeLuisa, A.; Doyle, B. P.; Gazzadi, G. C.; Giglia, A.; Finetti, P.; Mahne, N.; Pasquali, L.; Pedio, M.; Selvaggi, G.; Naletto, G.; Pelizzo, M. G.; Tondello, G. *AIP Conference Proceedings* **2004**, 708, 450.

(25) Grisham, M.; Vaschenko, G.; Menoni, C. S.; Rocca, J. J.; Pershyn, Y. P.; Zubarev, E. N.; Voronov, D. L.; Sevryukova, V. A.; Kondratenko, V. V.; Vinogradov, A. V.; Artioukov, I. A. *Optics Letters* **2004**, 29, 620.

(26) Gokhale, A. B.; Abbaschian, G. J. *Bull. Phase Diag.* **1986**, 7, 333-336.

(27) Eremenko, V. N.; Meleshevich, K. A.; Buyanov, Y. I.; Martsenyuk, P. S. *Powder Met. Met. Ceram.* **1988**, 967, 967-972.

(28) Kotroczo, V.; McColm, I. J. *Journal of Alloys and Compounds* **1994**, 203, 259.

(29) Lukashenko, G. M.; Polotskaya, R. I.; Sidorko, V. R. *Journal of Alloys and Compounds* **1992**, 179, 299.

(30) Siffalovic, P.; Majkova, E.; Chitu, L.; Jergel, M.; Luby, S.; Keckes, J.; Maier, G.; Timmann, A.; Roth, S. V.; Tsuru, T.; Harada, T.; Yamamoto, M.; Heunzmann, U. *Vacuum*, **2010**, 84, 19.

(31) de Boer D. K. G. *Physical Review B* **1995**, 51, 5297.

(32) Yulin S, Feigl T, Kuhlmann T, Kaiser N, Fedorenko AI, Kondratenko VV, Poltseva OV,

Sevryukova VA, Zolotaryov AY, Zubarev EN *Journal of Applied Physics* **2002**, 92, 1216.

(33) Pinegyn V, Zubarev EN, Kondratenko VV, Sevryukova VA, Yulin SA, Feigl T, Kaiser N *Thin Solid Films* **2008**, 516, 2973.

(34) Gösele U, Tu KN *Journal of Applied Physics* **1982**, 53, 3252.